Journal of Nuclear Medicine, published on October 18, 2019 as doi:10.2967/jnumed.119.234898

Intraindividual comparison of ^{18}F-PSMA-1007 with renally excreted PSMA ligands for PSMA-PET imaging in patients with relapsed prostate cancer

Brief Communication

Felix Dietlein[1,2], Carsten Kobe[1], Melanie Hohberg[1], Boris D. Zlatopolskiy[3], Philipp Krapf[4], Heike Endepols[1,3], Philipp Täger[1], Jochen Hammes[1], Axel Heidenreich[5], Thorsten Persigehl[6], Bernd Neumaier[3,4], Alexander Drzezga[1*] and Markus Dietlein[1* §]

[1] Department of Nuclear Medicine, University Hospital of Cologne, Germany
[2] Department of Medical Oncology, Dana-Farber Cancer Institute, Harvard Medical School, Boston, USA
[3] Institute of Radiochemistry and Experimental Molecular Imaging, University Hospital of Cologne, Germany
[4] Institute of Neuroscience and Medicine, INM-5: Nuclear Chemistry, Forschungszentrum Jülich GmbH, Germany
[5] Department of Urology, University Hospital of Cologne, Germany
[6] Institute of Diagnostic and Interventional Radiology, University Hospital of Cologne, Germany

* A.D. and M.D. contributed equally to this work.

§ **Corresponding author:** Markus Dietlein, Department of Nuclear Medicine, University Hospital of Cologne, Kerpener Str. 62, 50937 Cologne, Germany. Email: markus.dietlein@uk-koeln.de, Tel.: +49 221 478 5024, Fax: +49 221 478 89085

Running title: Comparison between PSMA PET tracers

Manuscript category: Brief communication

Keywords: prostate cancer, PET, PSMA tracer, ^{18}F-PSMA-1007, ^{68}Ga-PSMA-11, ^{18}F-DCFPyL, ^{18F}-JK-PSMA-7

Word count: abstract: 223; main text: 3,156

ABSTRACT

^{18}F-Prostate-specific membrane antigen (PSMA)-1007 is mainly excreted through the liver. We benchmarked the performance of ^{18}F-PSMA-1007 against three renally excreted PSMA-tracers.

Methods: Among 668 patients we selected 27 patients in whom the PET/CT with ^{68}Ga-PSMA-11, ^{18}F-DCFPyL, or ^{18}F-JK-PSMA-7 was interpreted as equivocal or negative or as oligometastatic disease (PET-1). Within <3 weeks, a second PET scan with ^{18}F-PSMA-1007 was performed (PET-2). The confidence in the interpretation of PSMA-positive loco-regional findings was scored on a 5-point scale, first in routine diagnostics (reader 1), then by an independent second evaluation (reader 2). Discordant PSMA-positive skeletal findings were examined by contrast enhanced MRI.

Results: For both readers, ^{18}F-PSMA-1007 facilitated the interpretability of 27 loco-regional lesions. In PET-2, the clinical read-out led to a significantly lower number of equivocal loco-regional lesions (p=0.024), reader 2 reported a significantly higher rate of suspicious lesions that were falsely interpreted as probably benign in PET-1 (p=0.023). Exclusively on PET-2, we observed a total of 15 PSMA-positive PSMA-spots in the bone marrow of 6 patients (= 22%). None of the 15 discordant spots had a morphological correlate on the corresponding CT or on the subsequent MRI. Thus, ^{18}F-PSMA-1007 exhibits a significantly higher rate of unspecific medullary spots (p=0.0006).

Conclusion: ^{18}F-PSMA-1007 may increase confidence to interpret small loco-regional lesions adjacent to the urinary tract. However, it may decrease the interpretability of skeletal lesions.

INTRODUCTION

Prostate-specific membrane antigen (PSMA)-PET/CT imaging is widely used for tumor localization in biochemical recurrence (BCR) of prostate cancer. A broad spectrum of PSMA ligands is now clinically available, including ^{68}Ga-PSMA-11, ^{18}F-DCFPyL, ^{18}F-JK-PSMA-7, and ^{18}F-PSMA-1007 (*1-6*). ^{18}F-JK-PSMA-7 is the PSMA-specific derivative 2-MeO-^{18}F-DCFPyL and proved non-inferior to ^{68}Ga-PSMA-11 in an intraindividual pilot study (*6,7*).

Most of the currently available PSMA tracers used for PET/CT imaging are excreted through the kidneys, thus leading to a high background signal in the urinary tract. It can therefore occasionally be difficult to differentiate between urine retention in the ureter and small adjacent pelvic lymph nodes. This ambiguity limits the reader's confidence in interpreting small PSMA-positive lesions close to the urinary tract as tumor relapse. Similarly, local recurrence close to the urinary bladder can be easily confused with urinary activity. Resolving this intrinsic limitation would bring us a step further towards exploiting the full potential of PSMA tracers.

Recently, the tracer ^{18}F-PSMA-1007 was introduced into clinical practice (*1,2*). In contrast to other PSMA tracers, ^{18}F-PSMA-1007 is excreted primarily through the liver. The pharmacodynamic study demonstrated that during the first 2 hours, only 1-2 % of the injected ^{18}F-PSMA-1007 activity was eliminated in the urine (*1*). Considerable hope is therefore being placed on ^{18}F-PSMA-1007 as a means of resolving the limited interpretability of PSMA-positive lesions near the urinary tract. A recent pilot study involving intraindividual comparisons reported that ^{18}F-PSMA-1007 and ^{18}F-DCFPyL detected the same lesions in 12 patients examined at initial staging (*8*).

Here, we present an intraindividual comparison of ^{18}F-PSMA-1007 with ^{68}Ga-PSMA-11, ^{18}F-DCFPyL, and ^{18}F-JK-PSMA-7 in 27 patients. We compared the readers' confidence in interpreting PSMA-positive lesions as tumor lesions, focusing on the interpretability of loco-regional lesions near the urinary tract. Additionally, we evaluated the performance of ^{18}F-PSMA-1007 in the whole-body PET scan.

MATERIALS AND METHODS

Patient characteristics

This observational study was approved and conducted in compliance with the Institutional Review Board. All patients gave their written informed consent to PET imaging and inclusion of their data in a retrospective analysis. All procedures were performed in compliance with the regulations of the responsible local authorities (District Administration of Cologne, Germany).

Patients with relapsed prostate cancer underwent PET/CT imaging with one of our routinely used PSMA tracers, ^{68}Ga-PSMA-11, ^{18}F-DCFPyL, or ^{18}F-JK-PSMA-7, as part of their clinical workup. A second PET/CT scan with ^{18}F-PSMA-1007 was performed in 27 cases (average age of 67.2±7.8 years) for one of the following three reasons: (i) the first PET scan was completely PSMA-negative; (ii) the first PET exhibited a PSMA-positive spot near the ureter, urethra, or bladder that was interpreted as equivocal; (iii) the first PET scan revealed a single suspicious lesion prior to metastasis-directed therapy (e.g.

radiotherapy). The second PSMA-PET/CT scan with ^{18}F-PSMA-1007 PET/CT was carried out within a period of 3 weeks following the first scan. The 27 patients were selected from an overall group of 668 patients who received PSMA PET/CT within the 12-month period of recruitment from April 2017 to March 2018. More details on patient characteristics are given in Supplemental table 1.

Imaging and reading

We performed PET/low dose CT imaging using standard activities and intervals between injection and start of data acquisition, as recommended for ^{68}Ga-PSMA-11 (n=16, average dosage 159±31 MBq), ^{18}F-DCFPyL (n=5, 343±52 MBq), and ^{18}F-JK-PSMA-7 (n=6, 323±54 MBq) (*4-6*). As in previous studies on ^{18}F-PSMA-1007 (*1,3*), we acquired ^{18}F-PSMA-1007 scans two hours after tracer injection with an average dosage of 343±49 MBq. All images were acquired on a Biograph mCT 128 Flow PET/CT scanner (Siemens Healthineers, Erlangen, Germany). The same filters and acquisition times (flow motion bed speed of 1.5 mm/sec) were used for the 4 PSMA ligands. Images were reconstructed using an ultra-high-definition algorithm.

The team of specialists in the routine diagnostics (two specialists in nuclear medicine and one radiologist, "reader 1") and one added reader ("reader 2") independently interpreted each PET/CT scan according to the criteria for harmonization of PSMA-PET/CT interpretation (*9*). "Reader 2" re-evaluated the PET scans without any knowledge of the clinical data or the MRI findings 3-15 months after the initial reading. We used the 5-point PSMA-RADS (reporting and data system) scale (version 1.0) to score the interpretability of each PSMA-positive lesion based on these reports. In particular, we classified each PSMA-positive finding as benign (PSMA-RADS-1), likely benign (PSMA-RADS-2), equivocal (PSMA-RADS-3), likely malignant (PSMA-RADS-4), or certainly malignant (PSMA-RADS-5), respectively (*10*).

Equivocal PSMA-positive lesions in the bone marrow were examined by dedicated, contrast enhanced MRI scans. Technical data on the MRI scans are provided in the Supplemental data.

Statistics

Statistical analyses were performed with Microsoft Excel, the R programming language and on vassarstats.net. We used Fisher's exact test (2x2 contingency tables), the Freeman-Halton extension (3x2 contingency tables) of Fisher's exact test and the Wilcoxon signed rank test to compare groups. To compare the shift in RDS categories, we combined categories 1 (almost certainly benign) and 2 (likely benign), as well as categories 4 (likely malignant) and 5 (almost certainly malignant), to obtain 3x2 contingency tables The interobserver variability was tested by the weighted Cohen's kappa test.

RESULTS

Interpretability of loco-regional PSMA-positive lesions

We performed the ^{18}F-PSMA-1007 PET in 27 patients who had been examined with ^{68}Ga-PSMA-11 (n=16), ^{18}F-DCFPyL (n=5), or ^{18}F-JK-PSMA-7 (n=6) less than 3 weeks previously (Figs. 1-3, Supplemental Figs. 1-4). For 8 of these 27 patients, the first PET did not reveal any loco-regional lesions. In these 8 patients, the second scan with ^{18}F-PSMA-1007 was negative in the loco-regional region as well (7 patients were entirely negative, one patient had an additional PSMA-positive bone marrow lesion on PET-1 and PET-2).

The remaining 19 patients were finally diagnosed with a PSMA-positive loco-regional tumor relapse when all imaging procedures were completed. In total, we identified 27 PSMA-positive loco-regional lesions in these patients. We then examined how interpretable these 27 PSMA-positive lesions were in both corresponding PET scans (PET-1: ^{68}Ga-PSMA-11, ^{18}F-DCFPyL, or ^{18}F-JK-PSMA-7; PET-2: ^{18}F-PSMA-1007). Reader 1 interpreted 15/27 lesions on PET scan 1 as equivocal (PSMA-RADS 3), whereas the fraction of equivocal lesions on PET scan 2 (^{18}F-PSMA-1007) was significantly lower (6/27 lesions, p=0.024, Fisher's exact test). For both readers, the rate of PSMA-positive lesions that were falsely interpreted as benign was lower on PET scan 2 (reader 1: 0/27, reader 2: 0/27) than on PET scan 1 (reader 1: 3/27, reader 2: 6/27), and this difference reached statistical significance for reader 2 (p=0.023). The rate of equivocal lesions did not differ significantly between the two scans for reader 2 (6 vs. 5 lesions, p=1.0). Overall, ^{18}F-PSMA-1007 exhibited a significant shift in PSMA-RADS categories towards higher confidence both for reader 1 (lower rate of equivocal ratings, p= 0.00154, Freeman-Halton extension of Fisher's exact test) and reader 2 (lower rate of falsely benign interpreted lesions, p=0.01745) (Table 1), suggesting that ^{18}F-PSMA-1007 enhanced the confidence in interpretation of loco-regional PSMA-positive lesions for both independent readers.

The ^{18}F-PSMA-1007 PET scan (PET-2) resulted in an almost perfect agreement, $\kappa = 0.95$ (weighted Cohen's kappa), while the interpretation of PET-1 led to a moderate agreement between the clinical read out and reader 2, $\kappa = 0.49$ (weighted Cohen's kappa). The data are shown in Supplemental table 2.

We next examined which aspects might have contributed to this improved interpretability. Concordantly, both readers corrected two false-positive interpretations of PSMA-spots in the pelvis from scan 1 (No. 2 and 24, cf. table 1) with the help of scan 2 (^{18}F-PSMA-1007) that was PSMA-negative in the finding of PET-1. Furthermore, the signal (SUV_{max}) of the 24 PSMA-positive lesions was significantly higher (p=0.00178, Wilcoxon signed rank test) on the ^{18}F-PSMA-1007 scan (average SUV_{max} 23.37±25.92) compared with the corresponding PET scan 1 (SUV_{max} 18.60±18.84). When comparing the signal between tracers separately, solely the difference between ^{68}Ga-PSMA-11 and ^{18}F-PSMA-1007 reached statistical significance (SUV_{max} 16.04±18.47 vs. 22.83±28.12, p=0.01367, 10 lesions). The differences between ^{18}F-DCFPyL and ^{18}F-PSMA-1007 (SUV_{max} 28.2±26.26 vs. 34.91±36.02, p=0.3125, 5 lesions) as well as JK-PSMA-7 and ^{18}F-PSMA-1007 (SUV_{max} 16.12±14.81 vs. 17.38±16.42, p=0.1641, 9 lesions) showed a similar trend but did not reach statistical significance.

The PSMA-positive lesions in the 19 patients were confirmed by histology in 5 patients, by follow-up in 11 patients and by morphological imaging in 1 patient. Follow-up data were not available for 2 patients. Further data for verification are presented in the Supplemental data and in Supplemental table 1.

Interpretability of PSMA-positive lesions in the bone marrow

We next compared the interpretability of osteo-medullary PSMA-positive lesions. Intriguingly, ^{18}F-PSMA-1007 detected a significantly higher number of PSMA-positive bone marrow findings compared with the other three tracers: while we identified 3 PSMA-positive bone marrow lesions on PET scans 1 (3/27 patients), ^{18}F-PSMA-1007 revealed a total of 18 PSMA-positive spots in 7/27 patients. Among these 7 patients, 4 patients exhibited only discrepant findings, 2 patients showed a combination of consistent and discrepant findings, and 1 patient had a concordant PSMA-positive skeletal lesion. Discordant results in the bone marrow were observed across all three tracers used for comparison (^{68}Ga-PSMA-11, 2 patients; ^{18}F-DCFPyL, 1 patient; ^{18}F-JK-PSMA-7, 3 patients).

The 3 PSMA-positive bone marrow lesions on PET scans 1 (^{68}Ga-PSMA-11, SUV_{max} 5.18±0.79) were also present on the corresponding scans with ^{18}F-PSMA-1007 (SUV_{max} 9.82±8.86). Furthermore, these 3 lesions had a morphological correlate on the corresponding CT scan (2 patients) or on a subsequent MRI scan (1 patient).

In marked contrast, none of the 15 findings that were exclusively detected with ^{18}F-PSMA-1007 had a morphological correlate on the corresponding CT scan. Due to this lack of a morphological correlate on the CT scan, both readers interpreted these 15 additional PSMA-positive spots as equivocal (PSMA-RADS category 3), although they had a high signal on the PET scan with an average SUV_{max} of 7.74±3.19, which was 7.07±2.52 and 4.11±2.91 times higher than the baseline SUV_{max} measured in the femoral head and in the thoracic aorta, respectively. This discrepancy resulted in a significant difference in PSMA-RADS categories between PET scans 1 and 2 ($p= 1.2893 \times 10^{-8}$, Freeman-Halton extension of the Fisher's exact test), and a significantly higher rate of equivocal findings (p=0.0006, Fisher's exact test). These lesions were subsequently double-checked through contrast-enhanced MRI imaging. All of these MRI scans were interpreted as unsuspicious in the bone marrow regions.

DISCUSSION

Our direct comparison of a first PET scan with ^{68}Ga-PSMA-11, ^{18}F-DCFPyL, or ^{18F}-JK-PSMA-7 with a second PET with ^{18}F-PSMA-1007 led to the following three major observations:

1.^{18}F-PSMA-1007 increased the readers' confidence in interpreting loco-regional PSMA-avid lesions near the ureter, the bladder or the urethra as tumor tissue when the previous PET scan with ^{68}Ga-PSMA-11, ^{18}F-DCFPyL, or ^{18}F-JK-PSMA-7 was read as equivocal. Furthermore, ^{18}F-PSMA-1007 PET imaging decreased the frequency of equivocal interpretations (routine diagnostics, "reader 1") or false-benign results ("reader 2"). Possible explanations are the lower background noise of ^{18}F-PSMA-1007 in the urinary tract as well as the higher signal of ^{18}F-PSMA-1007 in the loco-regional lesions. Although we observed this trend for all 3 tracers used for comparison, the difference in ^{18}F-PSMA-1007 signal reached statistical significance solely in comparison to ^{68}Ga-PSMA-11 (applies to 16/27 patients in our study

cohort). This might suggest that the ^{18}F label with its higher activity dose contributed more to our observation than ligand-specific factors.

2. Where the PET scan with ^{68}Ga-PSMA-11, ^{18}F-DCFPyL, or ^{18F}-JK-PSMA-7 was completely PSMA-negative in the pelvis, an additional PET scan with ^{18}F-PSMA-1007 did not reveal any additional loco-regional PSMA-positive lesions. All PSMA tracers examined in this study bind to the same protein domain, so that a lack of PSMA overexpression cannot be compensated by imaging with a second PSMA tracer.

3. Surprisingly, although not the primary goal of this study, we found that ^{18}F-PSMA-1007 exhibits a higher rate of unspecific focal bone marrow uptake compared with ^{68}Ga-PSMA-11, ^{18}F-DCFPyL, and ^{18}F-JK-PSMA-7. Since these additional bone marrow foci lacked morphological correlates in the corresponding low-dose CT scans, both readers interpreted these additional lesions as equivocal (PSMA-RADS category 3). The subsequent skeletal MRI scans were unsuspicious. We observed discrepant skeletal findings in 6 of our 27 patients (22%). Our results are concordant with a recent study that reported a higher rate of PSMA-positive bone marrow lesions in 102 patients examined with ^{18}F-PSMA-1007 compared with a matched-pair cohort examined with ^{68}Ga-PSMA-11 (*11*). However, in contrast to our study, these 102 patients received a scan with ^{18}F-PSMA-1007 only, and were not examined with a second PSMA tracer. In light of the results of our study, CT-negative bone marrow findings detected with ^{18}F-PSMA-1007 require validation by MRI scans. The importance of clinical follow-up is independent of the PSA value, since even patients with BCR and low PSA levels occasionally have PSMA-positive bone marrow metastases, as recently reported for ^{18}F-DCFPyL (*12*).

Limitations**:** Our direct comparison between ^{68}Ga-PSMA-11, ^{18}F-DCFPyL, and ^{18}F-JK-PSMA-7 in PET scan 1 and ^{18}F-PSMA-1007 in PET scan 2 was not designed as a prospective clinical trial. Readers were not blinded regarding the PSMA-PET tracers, and we observed a relevant inter-observer variability between readers 1 and 2 in the interpretation of PET-1 (weighted Cohen's $\kappa = 0.49$). Our observations were focused on a highly selected cohort of 27 patients from an overall group of 668 patients (= 4.0%) who underwent PSMA PET/CT during the recruitment period of one year. A second PSMA-PET scan with ^{18}F-PSMA-1007 was performed only when clinically indicated, mainly due to equivocal or negative interpretation of the first PET scan. For this reason, our cohort is relatively small. Establishing a preferred PSMA tracer will require independent validation in larger cohorts.

CONCLUSION

Our study suggests that choice of the right PSMA-tracer depends on the clinical context. ^{18}F-PSMA-1007 may increase confidence in interpreting small loco-regional lesions adjacent to the urinary tract, and may thus help to reduce equivocal interpretations in selected patients. However, ^{18}F-PSMA-1007 exhibits unspecific PSMA tracer accumulation in the bone marrow in a relevant number of patients. Thus, skeletal lesions detected with ^{18}F-PSMA-1007 require verification such as MRI or simultaneous

PET/MRI. Imaging with ^{18}F-PSMA-1007 may therefore be primarily applicable for patients with a high probability of locally restricted disease or as a follow-up test in cases with equivocal findings adjacent to the urinary tract. When searching for distant metastases, particularly in the bone marrow, ^{68}Ga-PSMA-11, ^{18}F-DCFPyL, or ^{18}F-JK-PSMA-7 may be more suitable, due to their higher specificity in the bone marrow.

DISCLOSURE

B.N., P.K., BD.Z., and A.D. have applied for a patent on ^{18}F-JK-PSMA-7. No other potential conflicts of interest relevant to this article exist.

KEY POINTS:

QUESTIONS: Does ^{18}F-PSMA-1007 exhibit a higher sensitivity for subtle differences near the urinary tract than other established PSMA tracers?
PERTINENT FINDINGS: ^{18}F-PSMA-1007 facilitated the interpretability of loco-regional PSMA-positive lesions compared with the other established PSMA-PET tracers. The number of equivocal and false-benign interpretations decreased significantly for two independent readers. However, ^{18}F-PSMA-1007 exhibits a substantial number of unspecific findings in the bone marrow.
IMPLICATIONS FOR PATIENT CARE: Due to the high tracer signal of the unspecific skeletal ^{18}F-PSMA-1007 spots, reader training alone will not solve this problem. Thus, skeletal lesions detected with ^{18}F-PSMA-1007 PET without a correlate in the corresponding CT require additional examination, such as MRI, or simultaneous PET/MRI.

REFERENCES

1. Giesel FL, Hadaschik B, Cardinale J, et al. F-19 labelled PSMA-1007: biodistribution, radiation dosimetry and histopathological validation of tumor lesions in prostate cancer patients. *Eur J Nucl Med Mol Imaging*. 2017;44:678-688.
2. Giesel FL, Knorr K, Spohn F, et al. Detection Efficacy of ^{18}F-PSMA-1007 PET/CT in 251 Patients with biochemical recurrence of prostate cancer after radical prostatectomy. *J Nucl Med*. 2019;60:362-368.
3. Rahbar K, Afshar-Oromieh A, Bögemann M, et al. ^{18}F-PSMA-1007 PET/CT at 60 and 120 minutes in patients with prostate cancer: biodistribution, tumour detection and activity kinetics. *Eur J Nucl Med Mol Imaging*. 2018;45:1329-1334.
4. Dietlein M, Kobe C, Kuhnert G, et al. Comparison of [(18)F]DCFPyL and [(68)Ga]Ga-PSMA-HBED-CC for PSMA-PET imaging in patients with relapsed prostate cancer. *Mol Imaging Biol*. 2015;17:575-584.
5. Dietlein F, Kobe C, Neubauer S, et al. PSA-stratified performance of (18)F- and (68)Ga-PSMA PET in patients with biochemical recurrence of prostate cancer. *J Nucl Med*. 2017;58:947-952.
6. Dietlein F, Hohberg M, Kobe C, et al. A novel ^{18}F-labeled PSMA ligand for PET/CT imaging of prostate cancer patients: First -in-man observational study and clinical experience with ^{18}F-JK-PSMA-7 during the first year of application. *J Nucl Med*. 2019;in press.
7. Zlatopolskiy BD, Endepols H, Krapf P, et al. Discovery of ^{18}F-JK-PSMA-7, a novel PET-probe for the detection of small PSMA positive lesions. *J Nucl Med*. 2019;60:817-823.
8. Giesel FL, Will L, Lawal I, et al. Intraindividual comparison of ^{18}F-PSMA-1007 and ^{18}F-DCFPyL PET/CT in the prospective evaluation of patients with newly diagnosed prostate carcinoma: a pilot study. *J Nucl Med*. 2018;59:1076-1080.
9. Eiber M, Herrmann K, Calais J, et al. Prostate cancer molecular imaging standardized evaluation (PROMISE): Proposed miTNM classification for the interpretation of PSMA-ligand PET/CT. *J Nucl Med*. 2018;59:469-478.
10. Rowe SP, Pienta KJ, Pomper MG, Gorin MA. Proposal for a structured reporting system for prostate-specific membrane antigen-targeted PET imaging: PSMA-RADS Version 1.0. *J Nucl Med*. 2018;59:479-485.
11. Rauscher I, Krönke M, König M, et al. Matched-pair comparison of ^{68}Ga-PSMA-11 and ^{18}F-PSMA-1007 PET/CT: frequency of pitfalls and detection efficacy in biochemical recurrence after radical prostatectomy. *J Nucl Med*. 2019;in press.
12. Wondergem M, Jansen BHE, van der Zant FM, et al. Early detection with 18F-DCFPyL PET/CT in 248 patients with biochemically recurrent prostate cancer. *Eur J Nucl Med Mol Imaging*. 2019;46:1911-1918.

TABLE

Reader 1	PET-2 (^{18}F-PSMA-1007)			
PET-1	PSMA-RADS	RADS 1 / 2	RADS 3	RADS 4 / 5
	1 / 2	0	0	3
	3	0	6	9
	4 / 5	0	0	9

Reader 2	PET-2 (^{18}F-PSMA-1007)			
PET-1	PSMA-RADS	RADS 1 / 2	RADS 3	RADS 4 / 5
	RADS 1 / 2	0	1	5
	RADS 3	0	4	2
	RADS 4 / 5	0	0	15

TABLE 1. Each of the two tables includes 27 lesions that were confirmed as PSMA true-positive loco-regional relapses. Reader 1 (table above) and reader 2 (table below) scored their confidence in interpreting the PSMA-positive lesions as a local tumor relapse on a 5-point scale (PSMA-RADS). The results of the PSMA-RADS rating are demonstrated by contingency tables. The ^{18}F-PSMA-1007 scan resulted in a significant shift of the PSMA-RADS categories, both for reader 1 (p= 0.00154, Freeman-Halton extension of Fisher's exact test) and reader 2 (p=0.01745), suggesting that ^{18}F-PSMA-1007 enhanced the interpretability of loco-regional PSMA-positive lesions for both independent readers.

Abbreviations: RADS, reporting and data system for imaging; PET-1, PET scan with ^{68}Ga-PSMA-11 or ^{18}F-DCFPyL or ^{18}F-JK-PSMA-7

FIGURES

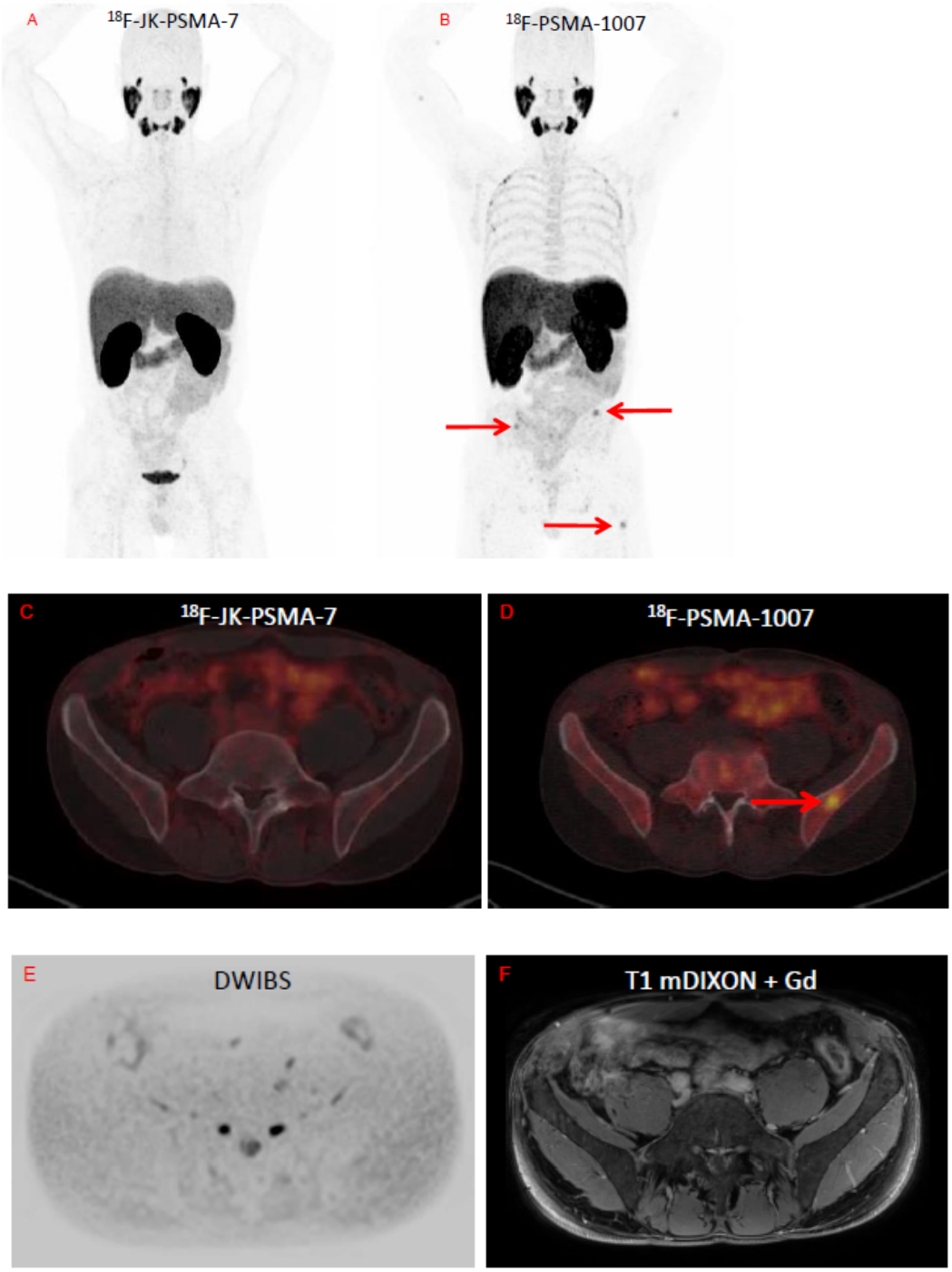

FIGURE 1. (A,C) ^{18}F-JK-PSMA-7 PET/low-dose CT on the left and (B,D) ^{18}F-PSMA-1007 PET/low-dose CT on the right of patient No. 21 with BCR. The histologically confirmed PSMA-positive lesion in the right seminal vesicle is shown in Supplemental Figure 1. The osteo-medullary spots with ^{18}F-PSMA-1007 in the left Os ilium (red arrows in B,F), in the right Os ilium (red arrow in B), and in the left femur (red arrow in B) did not have any correlate on the MRI scan (E,F). Biopsy, salvage prostatectomy, excellent PSA response.

Abbreviations: DWIBS, diffusion-weighted imaging with background body signal suppression; mDIXON FS, multi-point Dixon fat suppression

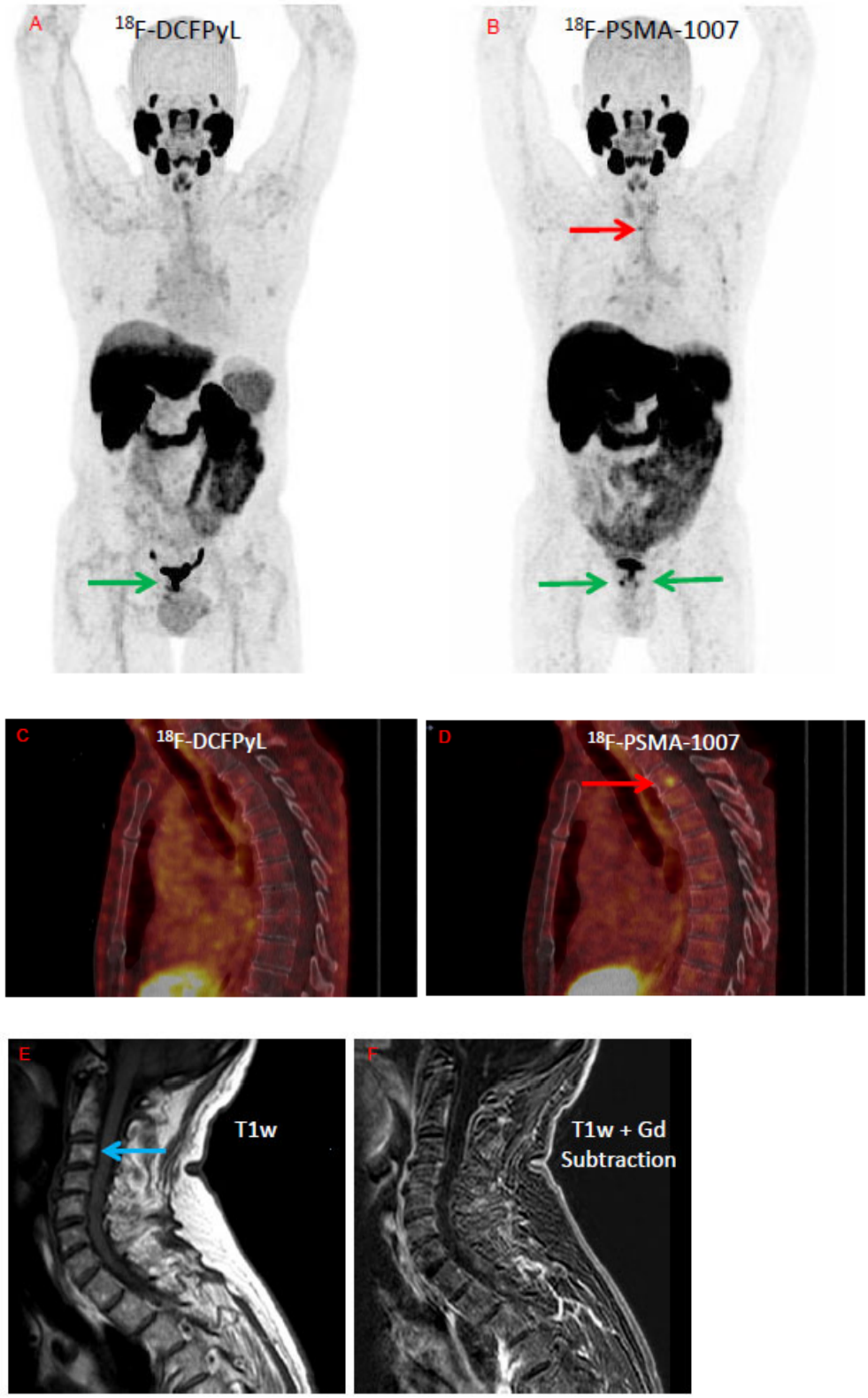

FIGURE 2. (A,C) ^{18}F-DCFPyL PET/low-dose CT on the left and (B,D) ^{18}F-PSMA-1007 PET/low-dose CT on the right of patient No. 13 with BCR. PSMA-positive intraprostatic lesions in the left and the right lobe of the prostate, visible with both ^{18}F-DCFPyL and ^{18}F-PSMA-1007 (green arrows in A,B). The osteo-medullary spots in the thoracic spine (Th 3, red arrows in B,D) did not have any correlate on the MRI scan (E,F). The hemangioma in the cervical spine 3 was PSMA-negative (blue arrow in E).

Abbreviations: Gd, Gadolinium

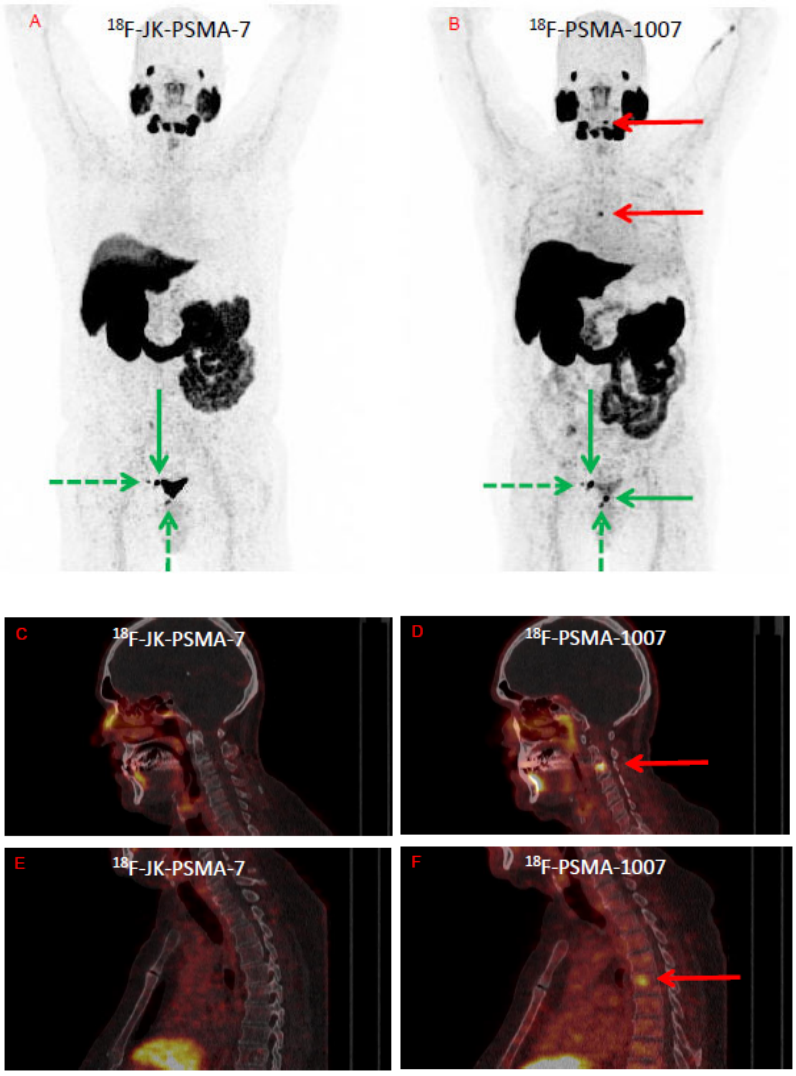

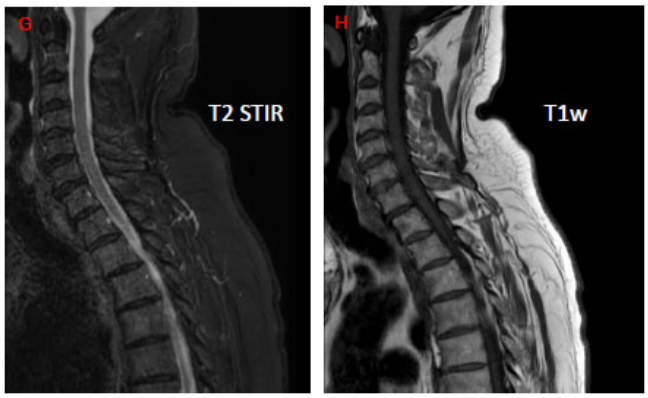

FIGURE 3. (A,C,E) ^{18}F-JK-PSMA-7 PET/low-dose CT on the left and (B,D,F) ^{18}F-PSMA-1007 PET/low-dose CT on the right of patient No. 27 with BCR. The maximum intensity projections (MIP) with ^{18}F-JK-PSMA-7 and ^{18}F-PSMA-1007 show two PSMA-positive lymph nodes right iliac and a PSMA-positive relapse below the bladder. Additionally, the ^{18}F-PSMA-1007 PET scan shows a further relapse localization at the junction between the bladder and the urethra (B). The osteo-medullary spots in the cervical spine (C3, red arrows in B,D) and thoracic spine (Th 5, red arrows in B,F) did not have any correlate on the MRI scan (G,H).

Abbreviations: T2 STIR, short T2 inversion recovery

Intraindividual comparison of ^{18}F-PSMA-1007 with renally excreted PSMA ligands for PSMA-PET imaging in patients with relapsed prostate cancer

Supplemental Data

Indication for PET/CT

Most patients (23/27) were referred to PET/CT imaging due to BCR according to the following criteria: PSA increase to 0.2 µg/l or more after prostatectomy (R0 or R1 resection); PSA increase of at least 2.0 µg/l above nadir after radiotherapy, as determined by the referring urologist. One patient revealed a persistent PSA level after prostatectomy. Additionally, we included 2 patients with oligometastatic disease and one patient with secondary neoplasia of rectal cancer for tissue differentiation. None of these patients received androgen deprivation therapy.

Tracer preparation

Synthesis of ^{18}F-PSMA-1007 was originally described by Giesel and colleagues (*1*) and performed at the Research Center Juelich on demand. All tracers were produced in accordance with applicable good manufacturing practice (*2*). The 11 batches of ^{18}F-PSMA-1007 for our 27 patients were produced at an average activity of 10.11±3.76 GBq, a specific activity of 318.09±235.15 GBq/µmol, an activity concentration of 986.91±358.97 MBq/ml, and a radiochemical purity of 99.0±0.77 %. Synthesis of ^{68}Ga-PSMA-11 (*3*), ^{18}F-DCFPyL (*2,4*), and ^{18}F-JK-PSMA-7 (*2*) was performed as described previously.

Technical data on the MRI scans

Equivocal PSMA-positive lesions in the bone marrow were examined by dedicated, contrast enhanced MRI scans. Technical data on the MRI scans is provided under Supplemental Data. MRI was performed at 1.5T and 3.0T MR scanners (Achieva and Ingenia, Philips Healthcare, Amsterdam, The Netherlands) using the clinical standard protocol by application of 0.1 mmol/ body weight GD-DOTA (Clariscan™, GE Healthcare Buchler, Braunschweig, Germany). Spine sequences: sagittal T2w, sagittal T2 STIR, sagittal T1w pre/post contrast injection and post-processing subtraction, and sequential transversal T2w and T1 SPIR. Pelvic sequences: Transversal T2 STIR, transversal DWIBS, coronal T2 STIR, coronal T1w pre/post contrast injection, and transversal T1 mDIXON FS.

Verification of the loco-regional PSMA-positive lesions

We followed up on the 19 patients with loco-regional PSMA-positive lesions to confirm that these lesions had a clinical correlate. For 5 patients, a histology report after salvage-lymphadenectomy (3 patients) or salvage-prostatectomy (1 patient) or biopsy (1 patient) was available. These histology reports directly verified the PSMA-positive lesions on the PET scan as prostate cancer tissue. For another 11 patients, follow-up data including PSA levels were available, and we observed a decrease in the PSA level

after radiotherapy (9 patients) or an increase in the PSA level (2 patients) in combination with progressive disease on a subsequent PSMA PET/CT after watchful waiting. We cross-validated the PSMA-positive lesions with a MRI scan of the pelvis in 1 patient. Follow-up data were not available in the remaining 2 patients. These 2 patients (no. 8 and no. 19 in Supplemental table 1) had previously undergone at least 2 PET scans and were already irradiated for PSMA-positive loco-regional recurrences. The PSMA-positive lesions in PET-1 and PET-2 were localized in these irradiated regions. Given this history, we found the PSMA-positive PET findings plausible.

No.	Indication	Gleason	PSA value	PSMA tracer used in PET-1	Lesions finally interpreted as PSMA true-positive (reader 1/ reader 2)		Lesions finally interpreted as PSMA false-positive or unspecific or urinary activity (reader 1/ reader 2)		Verification
					PET-1	PET-2	PET-1	PET-2	
1	Differen-tiation of local tissue (PCa vs. rectal cancer)	n.a.	10.5	^{18}F-JK-PSMA-7	T (RADS-4/ RADS-4) T (RADS-5/ RADS-5)	T (RADS-4/ RADS-4) T (RADS-5/ RADS-5)			Imaging (MRI of the pelvis)
2	Oligo-metastasis (after RT)	4+3	4.5	^{68}Ga-PSMA-11	M (RADS-5/ RADS-5)	M (RADS-5/ RADS-5)	N (RADS-3/ RADS-1)	Negative N (RADS-1/ RADS-1)	Imaging (skeletal CT), Follow-up 16 mo including PET/CT
3	BCR	3+4	1.26	^{68}Ga-PSMA-11	N (RADS-2/ RADS-2)*	N (RADS-4/ RADS-4)*			Histology (lymph nodes)
4	BCR	3+4	4.5	^{18}F-JK-PSMA-7	T (RADS-4/ RADS-4)	T (RADS-4/ RADS-4)			RT, Follow-up 9 mo including PET/CT
5	BCR	3+3	1.8	^{18}F-JK-PSMA-7	T (RADS-3/ RADS-4)	T (RADS-4/ RADS-4)			Follow-up 12 mo including PET/CT
6	Oligo-metastasis (before RT)	4+3	1.84	^{68}Ga-PSMA-11	T (RADS-3/ RADS-3) M (RADS-5/ RADS-5)	T (RADS-3/ RADS-4) M (RADS-5/ RADS-5)	Bone marrow in the additional regions PSMA-negative	M (RADS-3/ RADS-3) M (RADS-3/ RADS-3)	Skeletal MRI, skeletal RT, Follow-up 11 mo including PET/CT,

7	BCR	4+3	0.3	^{68}Ga-PSMA-11	T (RADS-3/ RADS-2)	T (RADS-4/ RADS-4)			RT, Stable disease 6 mo
8	BCR	4+3	27.7	^{68}Ga-PSMA-11	T (RADS-3/ RADS-4)	T (RADS-5/ RADS-5)			No follow-up data. PET/CT 7 and 15 mo before with loco-regional relapse
9	BCR	3+4	1.9	^{68}Ga-PSMA-11	T (RADS-3/ RADS-2)	T (RADS-4/ RADS-4)			RT, Follow-up 6 mo
10	BCR	3+4	1.5	^{18}F-DCFPyL	negative	negative			Follow-up 12 mo including serial PET/CT
11	BCR	4+5	1.9	^{68}Ga-PSMA-11	negative	negative			Small PSMA-negative lung metastases (histologically confirmed)
12	BCR	4+3	0.6	^{68}Ga-PSMA-11	negative	negative			Follow-up 9 mo
13	BCR	n.a.	4.3	^{18}F-DCFPyL	T (RADS-3/ RADS-2)	T (RADS-4/ RADS-4)	Bone marrow PSMA-negative	M (RADS-3/ RADS-3) M (RADS-3/ RADS-3) M (RADS-3/ RADS-3)	Skeletal MRI, RT, Follow-up 6 mo,
14	BCR	4+5	1.0	^{18}F-DCFPyL	N (RADS-2/ RADS-5)*	N (RADS-4/ RADS-4)*			Histology (lymph nodes)
15	BCR	4+5	2.1	^{68}Ga-PSMA-11	N (RADS-3/ RADS-4)	N (RADS-4/ RADS-4)			RT, Follow-up 6 mo.

16	BCR	3+4	1.59	^{68}Ga-PSMA-11	negative	negative			n.a.
17	BCR	n.a.	0.39	^{68}Ga-PSMA-11	negative	negative			MRI negative, RT, Stable disease 6 mo
18	BCR	3+3	0.71	^{68}Ga-PSMA-11	negative	negative			n.a.
19	BCR	4+5	7.7	^{18}F-DCFPyL	T (RADS-3/ RADS-5) N (RADS-3/ RADS-5)	T (RADS-5/RADS-5) N (RADS-5/ RADS-5)			No follow-up data. PET/CT 14, 30, and 46 mo before with loco-regional relapse
20	BCR	3+4	0.68	^{18}F-DCFPyL	T (RADS-4/ RADS-4)*	T (RADS-4/ RADS-4)*			Biopsy (local relapse)
21	BCR	4+3	1.76	^{18}F-JK-PSMA-7	T (RADS-3/ RADS-2)*	T (RADS-3/ RADS-3)*	Bone marrow PSMA-negative	M (RADS-3/ RADS-3) M (RADS-3/ RADS-3) M (RADS-3/ RADS-3)	Skeletal MRI, Biopsy, Histology (prostate)
22	Persistent PSA level after prostat-ectomy	4+3	3.9	^{68}Ga-PSMA-11	T (RADS-4/ RADS-4) M (RADS-3/ RADS-3)	T (RADS-4/ RADS-4) M (RADS-4/ RADS-4)	Bone marrow in the additional regions PSMA-negative	M (RADS-3/ RADS-3) M (RADS-3/ RADS-3) M (RADS-3/ RADS-3)	Skeletal MRI, RT prostate fossa and Th6, Follow-up 4 mo

23	BCR	n.a.	4.39	^{18}F-JK-PSMA-7	T (RADS-3/ RADS-3) T (RADS-3/ RADS-3)	T (RADS-3/ RADS-3 T (RADS-3/RADS-3)	Bone marrow PSMA-negative	M (RADS-3/ RADS-3)	Skeletal MRI, RT, Follow-up 3 mo
24	BCR	4+3	0.65	^{68}Ga-PSMA-11	N (RADS-5/ RADS-5)*	N (RADS-5/ RADS-5)*	T (RADS-3/RADS-3)	Negative T (RADS-1/ RADS-1)	Histology (lymph nodes)
25	BCR	3+5	0.8	^{68}Ga-PSMA-11	T (RADS-4/ RADS-4) T (RADS-3/ RADS-3)	T (RADS-4/ RADS-4) T (RADS-4/ RADS-4)			RT, Follow-up 3 mo
26	BCR	4+4	0.4	^{68}Ga-PSMA-11	negative	negative			n.a.
27	BCR	4+4	0.63	^{18}F-JK-PSMA-7	T (RADS-4/ RADS-4) T (RADS-1/ RADS-1) N (RADS-4/ RADS-4) N (RADS-3/ RADS-3) N (RADS-3/ RADS-3)	T (RADS-4/ RADS-4) T (RADS-4/ RADS-4) N (RADS-4/ RADS-4) N (RADS-3/ RADS-3) N (RADS-3/RADS-3)	Bone marrow PSMA-negative	M (RADS-3/ RADS-3) M (RADS-3/ RADS-3) M (RADS-3/ RADS-3)	Skeletal MRI, RT, Follow-up 3 mo

Supplemental Table 1. Data from the 27 patients, differentiating between finally established PSMA true-positive lesions and unspecific PSMA-positive spots. The PSMA-RADS categories are recorded for PET-1 with ^{68}Ga-PSMA-11, ^{18}F-DCFPyL, or ^{18}F-JK-PSMA-7 (reader 1/ reader 2) and for PET-2 with ^{18}F-PSMA-1007 (reader 1/ reader 2). Each registration describes one lesion: T: prostate, prostate fossa, or seminal vesicle; N: lymph node within the pelvis; M: findings in the bone or the bone marrow. The lesions with an asterisk (*) were histologically confirmed.

Abbreviations: BCR, biochemical recurrence; n.a., non-available; PCa, prostate cancer; RADS, reporting and data systems; RT, radiotherapy

PET-1	Reader 2			
Reader 1	PSMA-RADS	RADS 1 / 2	RADS 3	RADS 4 / 5
	1 / 2	2	0	1
	3	4	6	5
	4 / 5	0	0	9

PET-2 (^{18}F-PSMA-1007)	Reader 2			
Reader 1	PSMA-RADS	RADS 1 / 2	RADS 3	RADS 4 / 5
	RADS 1 / 2	0	0	0
	RADS 3	0	5	1
	RADS 4 / 5	0	0	21

Supplemental Table 2. Each of the two tables includes 27 lesions that were confirmed as PSMA true-positive loco-regional relapses. PET-1 (table above) and PET-2 (table below) were scored by two readers, who expressed their confidence in interpreting the PSMA-positive lesions as a local tumor relapse on a 5-point scale (PSMA-RADS). The interpretation of the ^{18}F-PSMA-1007 PET scans (PET-2) resulted in an almost perfect agreement, $\kappa = 0.95$ (weighted Cohen's kappa), while the interpretation of PET-1 led to a moderate agreement, $\kappa = 0.49$ (weighted Cohen's kappa).

Abbreviations: RADS, reporting and data system for imaging; PET-1; PET scan with ^{68}Ga-PSMA-11 or ^{18}F-DCFPyL or ^{18}F-JK-PSMA-7

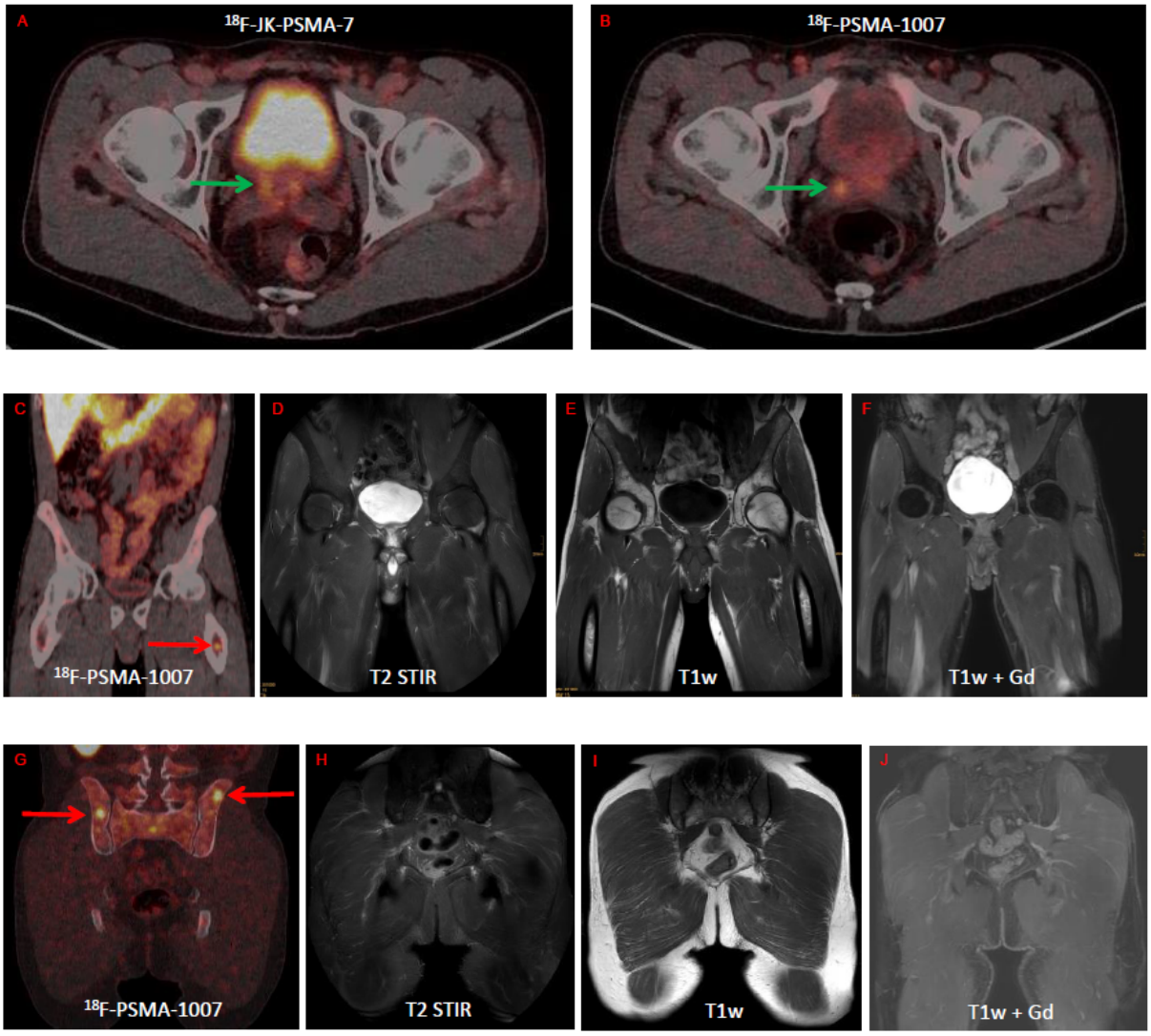

Supplemental Figure 1. (A) ^{18}F-JK-PSMA-7 PET/low-dose CT on the left and (B) ^{18}F-PSMA-1007 PET/low-dose CT on the right of patient No. 21 with BCR (same patient as in Fig. 1). The histologically confirmed PSMA-positive lesion in the right seminal vesicle is visible with both ^{18}F-JK-PSMA-7 and ^{18}F-PSMA-1007 (green arrows). The osteo-medullary spots with ^{18}F-PSMA-1007 in the left femur (red arrow in C), in the left Os ilium (red arrow in G), and right Os ilium (red arrows in G) did not have any correlate on the MRI scans (D-F and H-J).

Abbreviations: Gd, Gadolinium; T2 STIR, short T2 inversion recovery

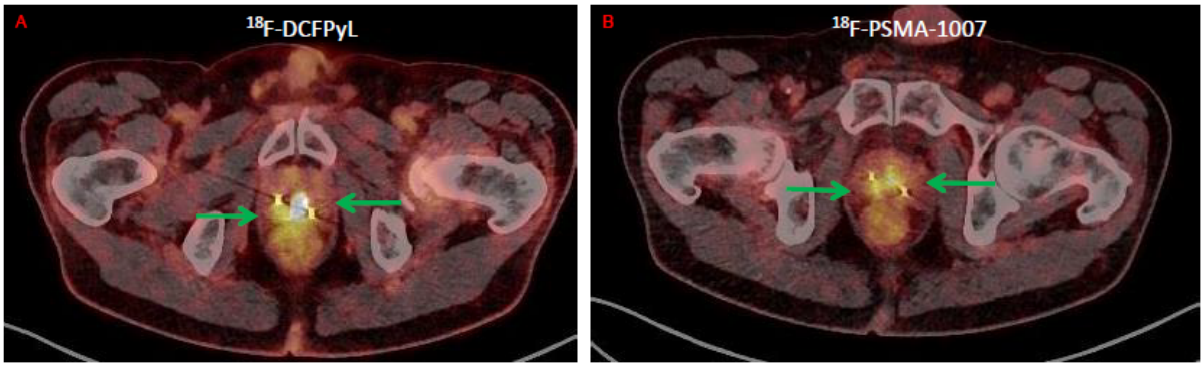

Supplemental Figure 2. (A) ^{18}F-DCFPyL PET/low-dose CT on the left and (B) ^{18}F-PSMA-1007 PET/low-dose CT on the right of patient No. 13 with BCR (same patient as in Fig. 2). PSMA-positive intraprostatic lesions in the left and the right lobe of the prostate, visible with both ^{18}F-DCFPyL and ^{18}F-PSMA-1007 (green arrows in A,B).

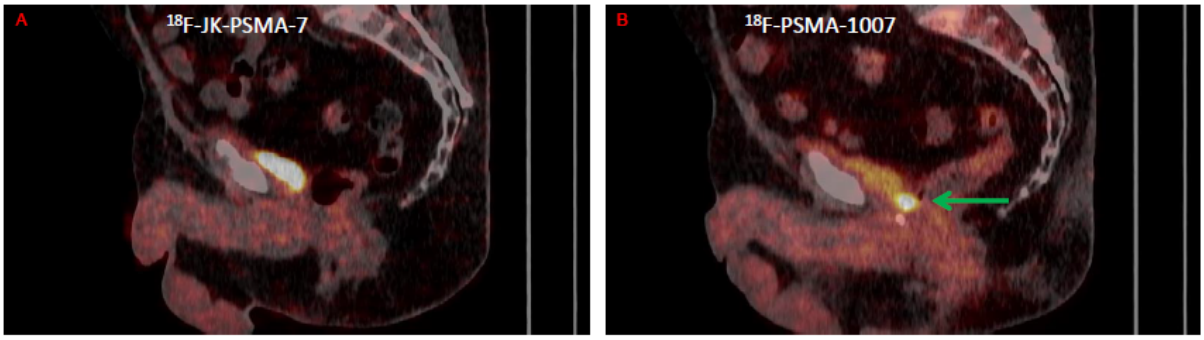

Supplemental Figure 3. (A) ^{18}F-JK-PSMA-7 PET/low-dose CT on the left and (B) ^{18}F-PSMA-1007 PET/low-dose CT on the right of patient No. 27 with BCR (same patient as in Fig. 3). The ^{18}F-PSMA-1007 PET scan (B) shows a further relapse localization at the junction between the bladder and the urethra.

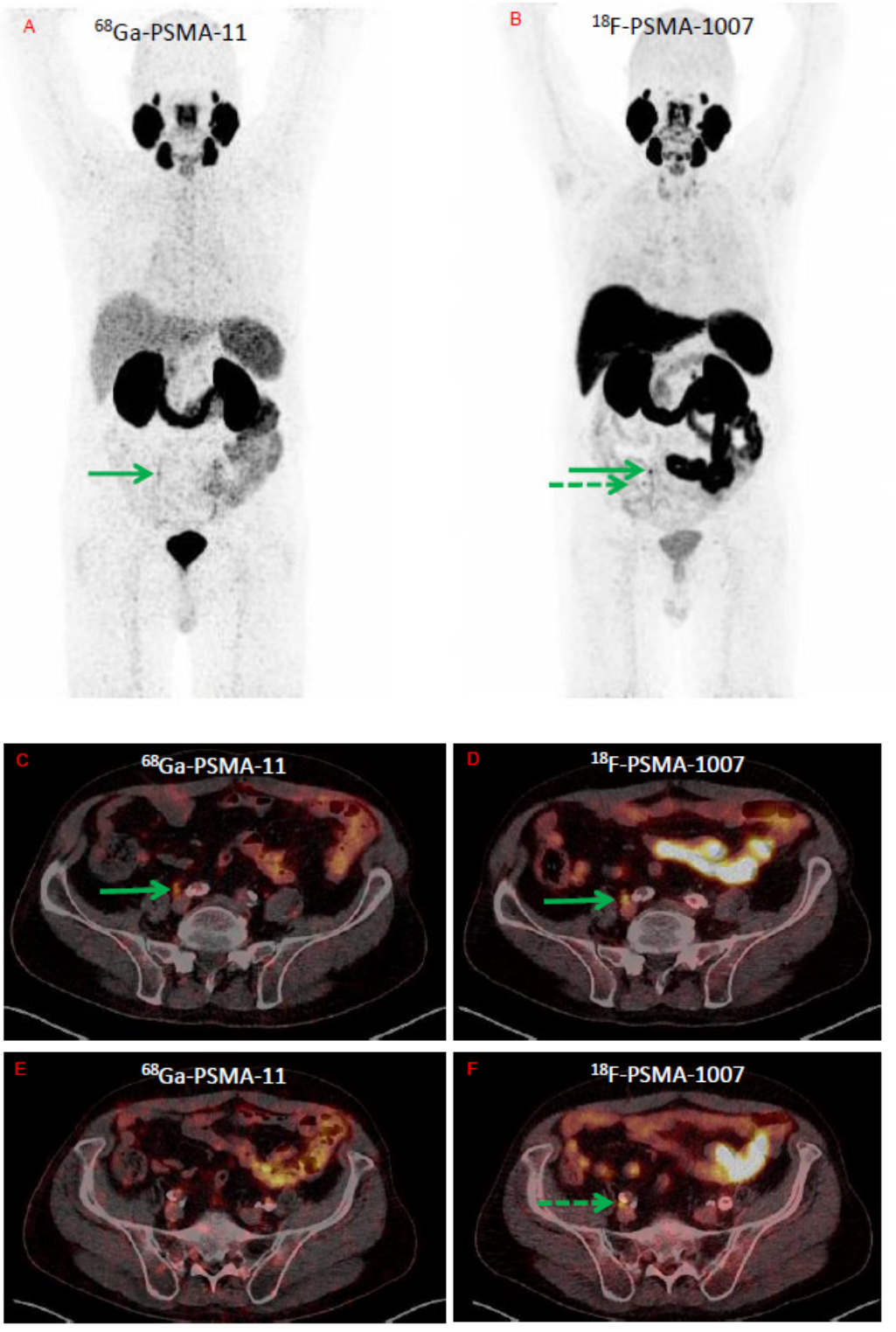

Supplemental Figure 4. (A,C,E) ^{68}Ga-PSMA-11 PET/low-dose CT on the left and (B,D,F) ^{18}F-PSMA-1007 PET/low-dose CT on the right of patient No. 3 with BCR. Two PSMA-positive lymph nodes very close to the right ureter (green arrows in A,B,C,D,F), the differentiation between a physiologic and a pathologic finding was difficult with the ^{68}Ga-PSMA-11 PET scan, but unequivocal with the ^{18}F-PSMA-1007 PET scan. Salvage lymphadenectomy, 3/7 histologically proven lymph node metastases.

References

1. Giesel FL, Hadaschik B, Cardinale J, et al. F-19 labelled PSMA-1007: biodistribution, radiation dosimetry and histopathological validation of tumor lesions in prostate cancer patients. *Eur J Nucl Med Mol Imaging*. 2017;44:678-688.
2. Zlatopolskiy BD, Endepols H, Krapf P, et al. Discovery of ^{18}F-JK-PSMA-7, a novel PET-probe for the detection of small PSMA positive lesions. *J Nucl Med*. 2019;60:817-823.
3. Eder M, Schafer M, Bauder-Wust U, et al. 68Ga-complex lipophilicity and the targeting property of a urea-based PSMA inhibitor for PET imaging. *Bioconjug Chem*. 2012;23:688-697.
4. Chen Y, Pullambhatla M, Foss CA, et al. 2-(3-{1-Carboxy-5-[(6-[18F]fluoro-pyridine-3-carbonyl)-amino]-pentyl}-ureido)-pen tanedioic acid, [18F]DCFPyL, a PSMA-based PET imaging agent for prostate cancer. *Clin Cancer Res*. 2011;17:7645-7653.